Original Article

Apolipoprotein E deficiency attenuated osteogenesis *via* down-regulating osterix

Qing Qi[1,2,3,§], Yingping Xu[4,§], Hongmei Sun[1,2,3], Jing Zhou[1,2,3], Lisha Li[1,2,3], Xinyao Pan[1,2,3], Jing Wang[1,2,3], Wenli Cao[5], Yan Sun[1,2,3,*], Ling Wang[1,2,3,*]

[1] Laboratory for Reproductive Immunology, Obstetrics and Gynecology Hospital of Fudan University, Shanghai, China;
[2] The Academy of Integrative Medicine of Fudan University, Shanghai, China;
[3] Shanghai Key Laboratory of Female Reproductive Endocrine-related Diseases, Shanghai, China;
[4] Reproductive Medicine Center, Taizhou Hospital Affiliated to Wenzhou Medical University, Linhai, Zhejiang, China;
[5] Reproductive Medicine Center of Zhoushan Maternal and Child Health Care Hospital, Zhoushan, Zhejiang, China.

SUMMARY   Apolipoprotein E (ApoE), a ligand for low-density lipoprotein receptors, is strongly induced during osteogenesis and has a physiologic role in regulating osteoblast function, but the mechanisms of its action are still unclear. The study aims to elucidate the influence and molecular mechanisms of *ApoE* on bone formation. An ovariectomy-induced osteoporotic model were conducted in *ApoE* knockout (*ApoE$^{-/-}$*) mice to study the effect of *ApoE* on the bone system. Bone quality were assessed through bone mineral density and histomorphometric analysis. To investigate the underlying role and mechanisms of *ApoE* during osteogenesis, primary osteoblasts from the calvariums of newborn *ApoE$^{-/-}$* or wild-type (WT) mice were cultured in the osteoblastic differentiation medium *in vitro* for further research. Our animal experiment data showed that *ApoE$^{-/-}$* mice exhibited bone loss, exacerbated by estrogen deprivation after ovariectomy. *ApoE* deficiency attenuated osteoblast activity and inhibited osteoblast osteogenesis, accompanied by decreased osterix expression. *ApoE* deficiency did not affect primary osteoblast viability and collagen-1 expression. Moreover, osteoprotegerin expression in *ApoE$^{-/-}$* osteoblasts was reduced compared to WT controls. Our study demonstrated that *ApoE* gene deficiency contributed to bone loss and attenuated osteogenesis by down-regulating osterix expression.

Keywords   apolipoprotein E, osteoblast, osteogenesis, osterix

1. Introduction

Osteoporosis and atherosclerosis are both prevalent diseases in postmenopausal women with bone and lipid metabolism disorders due to estrogen deficiency (*1*). Osteoporosis, characterized by decreased bone mass and density, could increase fracture risk, while atherosclerosis, characterized by dyslipidemia, is a syndrome affecting arterial blood vessels. Evidence notes that lipid metabolism is closely associated with bone metabolism. Recently, a study that included 1,116 Chinese female participants found that total cholesterol, low-density lipoprotein (LDL), and high-density lipoprotein (HDL) had a remarkable negative correlation with bone mass density at the lumbar spine (*2*). Another case-control study conducted with 150 individuals with metabolic syndrome has shown that vertebral fracture was a risk factor for coronary events (*3*). These studies imply that osteoporosis might share the same underlying pathogenesis as atherosclerosis.

Emerging evidence also shows that hyperlipemia might be a potent and important risk factor for osteoporosis (*4*). As we know, bone and fat originate from the same progenitor cell, multipotent mesenchymal stem cells (MSCs), which can differentiate into myoblasts or adipocytes under certain conditions (*5*). The products from LDL oxidation inhibit osteogenic differentiation and facilitate adipogenic differentiation of progenitor marrow stromal cells (*6,7*), resulting in osteoporotic bone loss. Oxidized lipids could regulate hyperlipidemia-induced parathyroid hormone resistance in bone anabolism in mice (*8*). Further on, in addition to their cholesterol-lowering effect, statins have been shown the bone anabolic action, indicating their protection against diseases such as osteoporosis (*9*). The pathogenesis of osteoporosis mainly results from the imbalance between osteoblasts and osteoclasts (*10,11*). Osteoblasts participate in bone formation while osteoclasts induce born absorption; bone formation could be hindered if disorders occur during osteoblasts' proliferation and

differentiation. Crosstalk between osteoblasts and osteoclasts is indispensable for maintaining the balance of bone metabolism (*11-13*). Osteoclastogenesis can be regulated by osteoblasts mainly through the receptor activator of the nuclear factor-κB (RANK) ligand (RANKL)/RANK/osteoprotegerin (OPG) axis (*14*).

Apolipoprotein E (ApoE), a significant plasma lipoprotein and a ligand for low-density lipoprotein receptors, is present in various tissues and expressed in different cells, including osteoblast, regulating the transportation and metabolism of lipids (*15*). Hyperlipidemia usually results from the gene mutations such as *ApoE*, which can be strongly induced during the mineralization of the primary osteoblasts *ex vivo* (*16*). Mice lacking *ApoE*, with a significant plasma cholesterol level, have displayed a high bone mass phenotype. In contrast, bone resorption was not affected due to an accelerated rate of bone formation (*16,17*). However, Hirasawa H *et al.* observed that *ApoE* knockout (*ApoE*$^{-/-}$) mice had reduced bone formation with a high-fat diet (*18*). Estrogen is a critical factor that could regulate both bone and lipid metabolisms. Estrogen decline during menopause causes lipid profile changes (*19*). Our previous study showed that estrogen could up-regulate the gene expression of *ApoE* receptors during osteoblast differentiation *in vitro* (*20*). The above observations indicated that *ApoE* might play a physiologic role in regulating osteoblast function, yet molecular mechanisms remained unclear.

In this work, *ApoE*$^{-/-}$ mice, which underwent ovariectomy or not, were conducted to probe the effect and underlying mechanisms of *ApoE* deficiency on the bone system. Bone mineral density (BMD) and histomorphometric parameters were analyzed to assess bone quality. To further investigate the relative mechanisms of bone metabolism regulated by *ApoE* deficiency, primary osteoblasts from newborn *ApoE*$^{-/-}$ and wild-type (WT) mice were cultured *in vitro*. Further experiments were carried out to explore mechanisms that *ApoE* deficiency regulates osteoblast-mediated osteoclastogenesis through RANKL/RANK/OPG axis.

2. Materials and Methods

2.1. Materials

The assay kits for total cholesterol (TC), LDL cholesterol, and HDL cholesterol were purchased from Nanjing Jiancheng Bioengineering Institute (Jiangsu, China). 4% paraformaldehyde (PFA) was purchased from Shanghai USEN Biological Technology Co., Ltd. (Shanghai, China). The tartrate-resistant acid phosphatase (TRAP) staining kit, calcein, β-glycerophosphate, ascorbate, dexamethasone, collagenase, 1α,25-(OH)$_2$ vitamin D$_3$ [1,25(OH)$_2$D$_3$], prostaglandin E2 (PGE2), and DMEM were obtained from Sigma-Aldrich, Inc. (St. Louis, MO, USA). Toluidine blue staining solution

was commercially obtained from Leagene Biotech Inc. (Beijing, China). Alpha minimum essential medium (α-MEM) medium, fetal bovine serum (FBS), and lipofectamine 2000 were obtained from Thermo Fisher Scientific Inc. (CA, USA). Dispase was purchased from F. Hoffmann-La Roche, Ltd. (Basel, Schweiz). Oricell^{TM} MSC osteogenic differentiation medium was bought from Cyagen Biosciences Inc. (Santa Clara, CA, USA). Penicillin, streptomycin, 5-bromo-4-chloro-3-indolyl-phosphate (BCIP)/nitroblue tetrazolium chloride (NBT), and MTT were obtained from Beyotime Biotech Inc. (Shanghai, China). The alkaline phosphatase (ALP) activity assay kit and Alizarin red S were purchased from GenMed Scientific Inc. (Shanghai, China). SYBR Premix Ex Taq II kits, RNAiso Plus, and PrimeScript RT Master Mix were commercially obtained from Takara Bio Inc. (Dalian, China). Si-*ApoE* and negative control (NC) were purchased from GenePharma Co., Ltd. (Shanghai, China). OPG was purchased from USCN Life Sciences Inc. (Wuhan, China). Primary antibodies against runt-related transcription factor 2 (Runx2), osterix, β-actin, and collagen-1 were purchased from Abcam Plc. (Cambridge, UK).

2.2. Animals

ApoE$^{-/-}$ and WT mice with C57BL/6 genetic background, aged 10-12 weeks, were commercially acquired from the Shanghai laboratory animal center of the Chinese Academy of Sciences (Shanghai, China). The mice were housed in a humidity-controlled (43 ± 8%) and temperature-controlled (23 ± 0.5℃) environment with a 12 h light and 12 h dark cycle. The Ethics Committee of Fudan University permitted the experimental protocols (approval number JS-020), which were carried out following the guidelines of Fudan University and the National Institutes of Health Guide for the Care and Use of Laboratory Animals.

Mice were mated with the same genotype, and newborn mice (2 days old) were used to isolate primary osteoblasts. *ApoE*$^{-/-}$ and WT mice (8 weeks old) were divided into four groups: ovariectomized (OVX) WT group, OVX *ApoE*$^{-/-}$ group, sham WT group, and sham *ApoE*$^{-/-}$ group (*n* = 6 for each group). Mice in the two OVX groups underwent ovariectomy through bilateral incisions, while mice in the two sham groups underwent the same surgical procedure without ovariectomy. After 12 weeks, murine blood, femur, and tibia sample were collected and analyzed.

2.3. Assessment of serum lipid profiles

Peripheral blood samples were collected from isoflurane-anesthetized mice by cardiac puncture to prepare the serum. Serum TC, LDL cholesterol, and HDL cholesterol were evaluated with a HITACHI-7080 automatic biochemical analyzer (Hitachi High-Tech Corporation,

Tokyo, Japan).

2.4. BMD and histomorphometric analysis

Dual-energy X-ray absorptiometry (DXA) was conducted to determine BMD with an animal PIXImus densitometer (Lunar; GE Corp., Fairfield, CT, USA), which the same technician performed. Uniformity was conducted by selecting consistent regions of interest from each sample for analysis. Bone structural parameters were detected with micro-computed tomography (micro-CT, Skyscan 1176, Bruker Corporation, Massachusetts, USA).

2.5. Immunohistochemistry

As previously described (*21*), after being fixed in 4% PFA, the murine tibiae were proceeded for decalcification with ethylenediaminetetraacetic acid, staining with TRAP for osteoclasts identification; the fixed murine tibiae were then stained with toluidine blue for analysis. Histological changes were observed using a microscope (Olympus, Tokyo, Japan).

2.6. Calcein labeling analysis

The bone formation sites were labeled with calcein referred to previous methods. Briefly, mice were administrated with calcein through intraperitoneal injection 7 and 2 days before the end of the experiment (*21*). Two nonconsecutive sections were collected from the tibia to measure bone formation rate (BFR) and mineral apposition rate (MAR) with a fluorescence microscopy (Olympus BX-60, Tokyo, Japan). The parameters, including BFR and MAR were analyzed referring to the previous protocols (*22*).

2.7. Primary osteoblasts isolation and differentiation

According to the genotype, primary osteoblasts were isolated from the calvaria of the newborn *ApoE*$^{-/-}$ and WT mice (*23*). Skull bones were digested five times (10 min each time) in α-MEM medium supplemented with 0.5% dispase and 0.1% collagenase. The first digestion was discarded; cells were collected from the remainder of the digestion and cultured in complete α-MEM for further study. The cell density in 24-well or 6-well culture plates is 5×10^4 per well or 1×10^5 per well, respectively. When cells reached 80% confluence, osteoblasts differentiation was induced in Oricell^{TM} MSC osteogenic differentiation medium with ingredients from the kit as follows: MSC osteogenic differentiation basal medium supplemented with 10% MSC-qualified FBS, 1 M β-glycerophosphate, 20 mM ascorbate, and 1 mM dexamethasone.

2.8. ALP staining and activity analyses

Cells in 24-well plates were used for ALP staining, and cells in 6-well plates were used for ALP activity analyses after treating osteogenic differentiation medium for seven days. BCIP/NBT is the preferred staining substrate for ALP detection, and we performed ALP staining referring to the manufacturer's instructions. According to the protocol, an alkaline phosphatase activity assay kit was used to detect ALP activity in cell lysate. The pictures were obtained with a microscope (Nikon Corporation, Tokyo, Japan).

2.9. Alizarin red S staining

The calcium deposits of differentiated primary osteoblasts in 24-well culture plates were stained using Alizarin red S according to the provided protocol after osteogenic induction medium treatment for 21 days (*23*). Then the number of bone nodules was observed with a microscope (Nikon Corporation) and counted.

2.10. Proliferation analysis

1×10^3 per well primary osteoblasts were seeded into 96-well plates to perform MTT assay to monitor cell viability. The medium was exchanged with the MSC osteogenic differentiation medium when cells were fully adherent. 0.5 mg/mL MTT reagent was added separately after 12, 24, 48, and 96 h and incubated at 37°C for 4 h. The precipitation was dissolved in dimethyl sulfoxide after the supernatant was gently removed. Absorbance at 490 nm was determined with an enzyme-linked immunometric meter (Bio-Tek 800, Agilent Technologies, Inc., CA, USA).

2.11. RNA isolation and reverse transcription-quantitative PCR (qRT-PCR)

Primary osteoblasts were cultured in 6-well culture plates for 0, 3, 7, and 21 days, and then cells were collected to detect the gene expression. Primary osteoblasts were cultured for seven days and sequentially treated with or without 10^{-6} M 1,25(OH)$_2$D$_3$ and 10^{-8} M PGE2 for 0, 1, and 2 days; the cells were used to detect the gene expression. Total RNA was extracted with an RNAiso Plus, referring to the provided protocol. Reverse transcription of total RNA was handled with a PrimeScript RT reagent kit. Quantitative PCR was conducted on Applied Biosystems 7900 HT (Thermo Fisher Scientific Inc.). Gene expression was analyzed with the $2^{-\Delta\Delta CT}$ method. The used primers are listed in Table 1.

2.12. Cell line MC3T3-E1 culture and transfection

MC3T3-E1, a mouse osteoblastic cell line, was commercially acquired from American Type Culture Collection (ATCC; Rockville, MD, USA) and cultured in DMEM with 10% FBS. For further research, MC3T3-E1

Table 1. The used primers are listed

Gene	Forward Primer	Reverse Primer
Runx2	GACAGTCCCAACTTCCTGTG	GCGGAGTAGTTCTCATCATTC
Osterix	GCTCGTAGATTTCTATCCTC	CTTAGTGACTGCCTAACAGA
Collagen-1	TGACTGGAAGAGCGGAGAGTA	GACGGCTGAGTAGGGAACAC
Opg	CCTTGCCCTGACCACTCTTAT	CGCCCTTCCTCACACTCAC
Rankl	CAAGATGGCTTCTATTACCTGT	TTGATGCTGGTTTTAACGAC
β-actin	CCTCTATGCCAACACAGT	AGCCACCAATCCACACAG

Opg: Osteoprotegerin; Rankl: Receptor activator of the nuclear factor-κB ligand; Runx2: Runt-related transcription factor 2.

was cultured in MSC osteogenic differentiation medium and transfected with si-*ApoE* or NC using Lipofectamine 2000. Cells were lysed to extract protein for western blot.

2.13. Western blot analysis

Cell protein samples were isolated, quantified, and denatured in sequence. The insoluble debris was removed by centrifugation, and the supernatant was retained for western blot analysis. Proteins were separated by electrophoresis on 10% sodium dodecyl sulfate polyacrylamide gels and transferred to a Hybond membrane. The membranes were blocked with non-fat milk, followed by incubation with primary antibodies against Runx2, osterix, collagen-1, and β-actin overnight at 4°C. They are rinsed in a washing buffer three times and subsequently incubated with secondary antibodies. Signals were detected using a chemiluminescence system and displayed on an Amersham Imager 600 (GE Healthcare Life Sciences, MA, USA).

2.14. Enzyme-linked immunosorbent assay (ELISA)

Primary osteoblasts were cultured in the MSC osteogenic differentiation medium for seven days and then incubated with or without $1,25(OH)_2D_3$/PGE2 for 1 and 2 days. The culture supernatants were collected and used to detect the concentrations of OPG in accordance with the manufacturer's protocol.

2.15. Statistical analysis

Data were presented as the mean ± SEM. One-way ANOVA was performed followed by Bonferroni-Holm-adjusted *post-hoc* comparisons among three or more groups. The student's *t*-test was applied between two groups. $p < 0.05$ represented a significant difference.

3. Results

3.1. Bone loss was exacerbated in *ApoE*-deficient mice

Since deficiency of the *ApoE* gene is critical in cholesterol transport in mice, we first assessed serum lipid profiles. $ApoE^{-/-}$ mice showed a significantly increased serum TC and LDL cholesterol but reduced

HDL cholesterol levels (Figure 1A), in accordance with a previous study (*18*). Ovariectomy did not affect serum levels of TC, LDL, and HDL (Figure 1A). To further explore femoral bone histomorphometric changes in *ApoE*-deficient mice, micro-CT analysis was performed to analyze bone properties. In the two sham groups, decreased BMD was observed in the bone trabecula of $ApoE^{-/-}$ mice but not WT mice (Figure 1B-1C left); in the two OVX groups, *ApoE* deprivation exacerbated the decrease in trabecular BMD compared to the WT mice (Figure 1B-1C left); OVX $ApoE^{-/-}$ mice had a lowest trabecular BMD in the four groups (Figure 1B, 1C left). Cortical BMD remained indistinguishable among the four groups, indicating ovariectomy or *ApoE* deficiency didn't affect cortical BMD (Figure 1B-1C right). Ovariectomy resulted in a decreased trabecular BMD, bone volume/tissue volume (BV/TV) ratio (Figure 1D), trabecular thickness (Tb.Th, Figure 1E), trabecular number (Tb.N, Figure 1G), and a remarkable increase in trabecular separation (Tb.Sp, Figure 1F), indicating a bone loss after estrogen deprivation through ovariectomy. Interestingly, *ApoE* deficiency aggravated the reduction of the BV/TV ratio, Tb.Th, and Tb.N and improved the Tb.Sp value (Figure 1C-G). OVX $ApoE^{-/-}$ mice had the lowest values of the BV/TV ratio, Tb.Th, and Tb.N and the highest Tb,Sp value in the four groups (Figure 1C-1G), showing *ApoE* deficiency aggravated bone loss.

To further explore the effects of *ApoE* deficiency on bone tissue homeostasis, we detected the static and bone dynamic histomorphometric parameters. The number of osteoblasts and osteoclasts were both increased in OVX mice, along with elevated BFR (Figure 1J, 1M) and MAR (Figure 1J, 1N), compared to the sham control mice; however, *ApoE* deficiency significantly reduced the number of osteoblasts (Figure 1H, 1K), BFR values (Figure 1J, 1M), and MAR values (Figure 1J, 1N). In contrast, the number of osteoclasts remained indistinguishable between WT and $ApoE^{-/-}$ mice (Figure 1I, 1L). These results indicated that *ApoE* deficiency resulted in osteopenia, possibly due to reduced osteoblastogenesis.

3.2. *ApoE* deficiency attenuated osteoblast activity and inhibited mineralization of differentiated primary osteoblasts
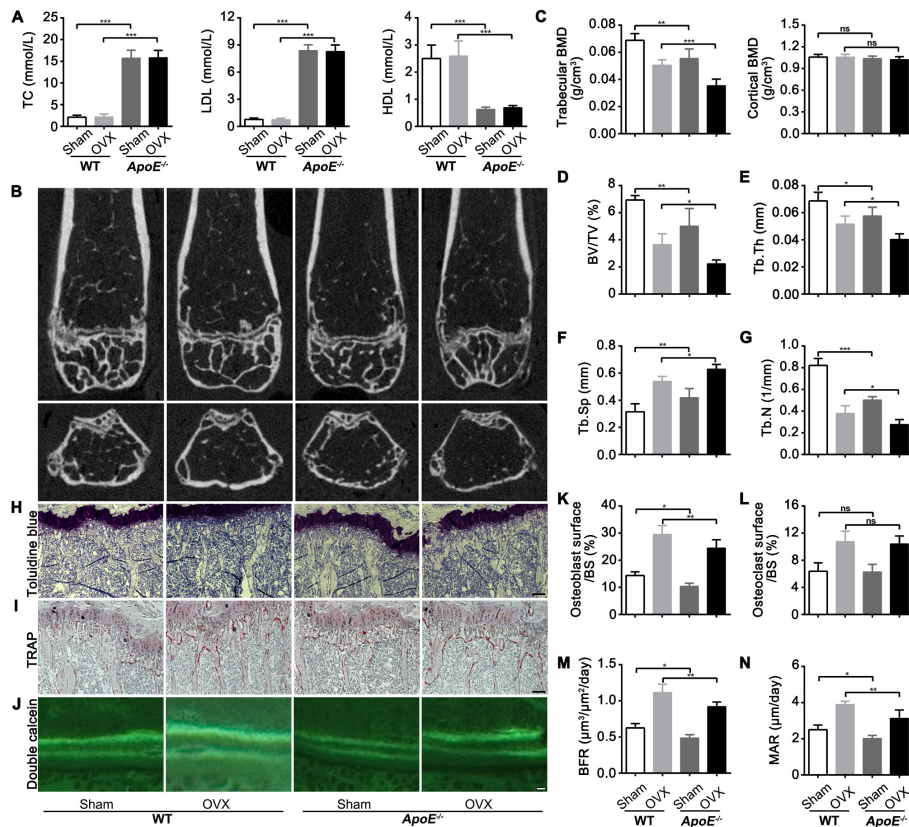
Figure 1. *ApoE* deficiency enhanced ovariectomy-induced bone loss. Eight-week-old mice underwent ovariectomy in OVX *ApoE^-/-* and OVX WT groups; mice in sham *ApoE^-/-* and sham WT groups underwent the same surgical procedure without ovariectomy. *n* = 6 for each group. After 12 weeks, all mice were sacrificed; serum and bone tissues were harvested for further investigation. **(A)** Serum levels of TC, LDL, and HDL. DXA was performed to measure trabecular and cortical BMD in each group. Micro-CT was used to determine the femoral phenotype in each group. **(B)** Micro-CT images. **(C)** Trabecular BMD and cortical BMD of femora. **(D)** BV/TV ratio, **(E)** Tb.Th, **(F)** Tb.Sp, and **(G)** Tb.N were measured. Histological analysis of the proximal tibiae in each group: **(H)** Toluidine blue staining, **(I)** TRAP staining, and **(J)** double calcein labeling. **(K)** Osteoblast surface/BS (%), **(L)** osteoclast surface/BS (%), **(M)** BFR, and **(N)** MAR were measured using the Osteo-Measure Histomorphometry System. **(H-I)** Scale bar represents 50 μm. **(J)** Scale bar represents 2 μm. Values are presented as the mean ± SEM. *$p < 0.05$, **$p < 0.01$, ***$p < 0.001$.
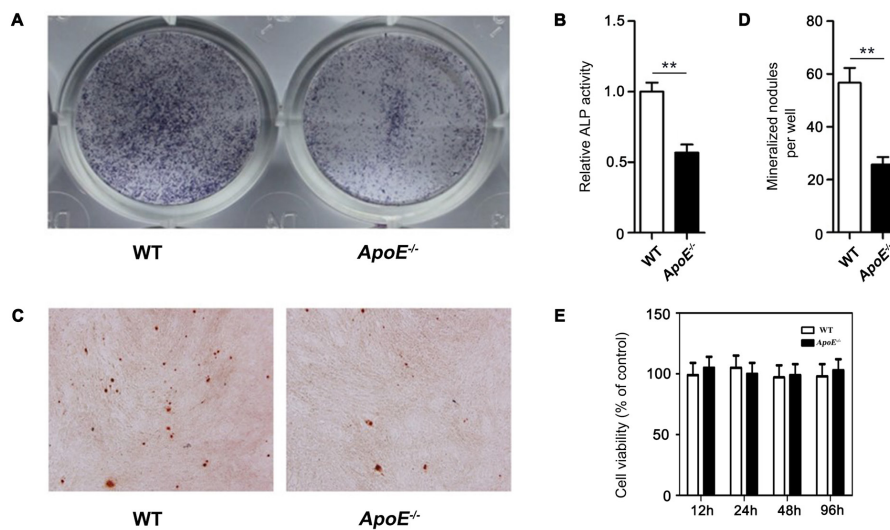

Figure 2. *ApoE* deficiency attenuated osteoblast activity and inhibited the mineralization of differentiated osteoblasts. Primary osteoblasts from *ApoE^-/-* and WT mice were treated with an MSC osteogenic differentiation medium. After osteogenic induction for seven days, **(A)** ALP staining was used to evaluate osteoblast activity; **(B)** the quantitative analysis of ALP activity in cell lysate was determined using an ALP activity analysis kit. **(C)** Alizarin Red S staining was performed after osteogenic induction for 21 days, and **(D)** the number of mineralized nodules per well was calculated. **(E)** MTT assay was conducted to detect the cell viability of primary osteoblasts after being cultured with an osteogenic differentiation medium for 12, 24, 48, and 96 h. Values are presented as the mean ± SEM of at least three experiments. **$p < 0.01$.
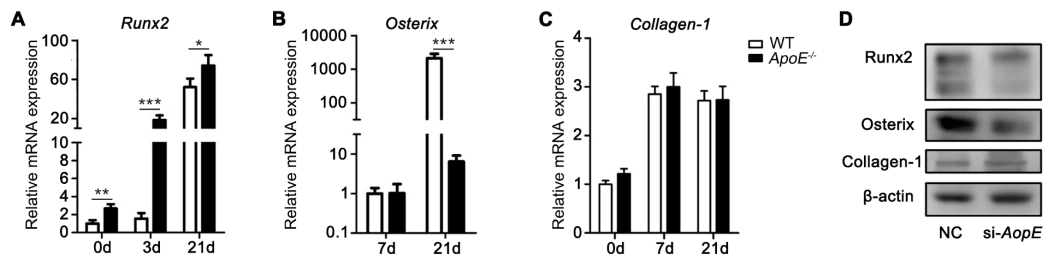
Figure 3. *ApoE* deficiency impaired the expression of osterix. Primary osteoblasts were cultured in an osteogenic induction medium for 0, 3, 7, and 21 days. Cells were harvested for total RNA extraction, and qRT-PCR was performed to analyze the gene expression. **(A)** *Runx2* mRNA expression. **(B)** *Osterix* mRNA expression. **(C)** *Collagen-1* mRNA expression. Values are presented as the mean ± SEM. **(D)** Western blot was performed to analyze protein levels of Runx2, osterix, and collagen-1 in mouse osteoblastic cell line MC3T3 after transfection with NC or si-*ApoE*. $*p < 0.05$, $**p < 0.01$, $***p < 0.001$.

To explore mechanisms of *ApoE* deficiency affecting bone metabolism, primary osteoblasts from *ApoE$^{-/-}$* and WT mice were cultured in MSC osteogenic differentiation medium. ALP staining was conducted to evaluate the ALP activity of osteoblasts. Fewer blue spots showed that the ALP activity of *ApoE$^{-/-}$* osteoblasts decreased compared to the osteoblasts from WT mice (Figure 2A). Meanwhile, ALP activity in the cell lysate from *ApoE$^{-/-}$* osteoblasts was also significantly reduced (Figure 2B). As shown in Figure 2C-2D, the number of osteoblastic calcium nodules in *ApoE$^{-/-}$* osteoblasts was less than that in osteoblasts from WT controls, indicating that *ApoE* deficiency suppressed bone formation *in vitro*. In addition, to explore whether *ApoE* deficiency can affect the proliferation activity of the osteoblasts, an MTT assay was conducted to detect cell activity on the primary osteoblasts from WT and *ApoE$^{-/-}$* mice *in vitro*. Data showed that *ApoE* deficiency had no noticeable impact on the cell viability of osteoblasts (Figure 2E).

3.3. *ApoE* deficiency inhibited the expression of osterix during the late stage of osteoblast differentiation *in vitro*

Osterix and Runx2 are key transcriptional factors during osteoblast differentiation; Runx2 is an early molecular regulator, whereas osterix is expressed in the late stage of osteoblast differentiation (*24,25*). Osteoblast differentiation was induced *in vitro* to assess the relative gene levels. Results demonstrated that the mRNA expression levels of *Runx2* in osteoblasts from *ApoE$^{-/-}$* mice were higher on days 0, 3, and 21 compared to WT controls (Figure 3A). The *osterix* mRNA expression in osteoblasts from *ApoE$^{-/-}$* mice was down-regulated on day 21, but there was no significant change on day 7 (Figure 3B). Meanwhile, the osterix protein expression in the si-*ApoE* group was reduced (Figure 3D), agreeing with the tendency of the reduced mRNA level. As shown in Figure 3C-3D, we didn't observe a noticeable difference in collagen-1 expression between *ApoE$^{-/-}$* and WT osteoblasts.

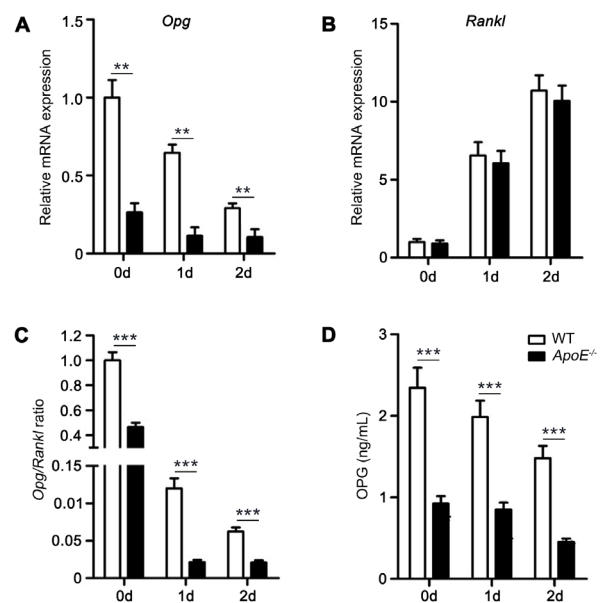**3.4. *ApoE* deficiency down-regulated OPG expression and *Opg/Rankl* ratio**

Figure 4. *ApoE* deficiency down-regulated OPG expression and *Opg/Rankl* ratio without affecting *Rankl* expression of osteoblasts *in vitro*. Primary osteoblasts cultured in the osteogenic differentiation medium were treated with or without $1,25(OH)_2D_3$/PGE2. After 0, 1, and 2 days, cells were harvested for total RNA extraction, and qRT-PCR was conducted to analyze the expression of **(A)** *Opg* and **(B)** *Rankl*. **(C)** The *Opg/Rankl* ratio. **(D)** Cell supernatant was used to test the protein level of OPG by ELISA analysis. Values are presented as the mean ± SEM of at least three experiments. $**p < 0.01$, $***p < 0.001$.

Osteoblasts can regulate osteoclast differentiation by expressing OPG and RANKL through the RANKL/RANK/OPG system, a vital signaling pathway involved in osteoclastogenesis. Primary osteoblasts from *ApoE$^{-/-}$* and WT mice were treated with $1,25(OH)_2D_3$/PGE2. A notable reduction in the *Opg* mRNA level was observed in osteoblasts from *ApoE$^{-/-}$* mice (Figure 4A), whereas *ApoE* deficiency did not affect the *Rankl* mRNA level (Figure 4B). However, the ratio of *Opg/Rankl* significantly decreased in *ApoE$^{-/-}$* osteoblasts compared to WT controls (Figure 4C). Moreover, the OPG protein level in the supernatant of *ApoE$^{-/-}$* osteoblasts was remarkably reduced, indicating *ApoE* deficiency might affect the function of osteoblasts (Figure 4D).

4. Discussion

Our study focused on the role and related mechanisms of *ApoE* deficiency on bone metabolism at both animal and cellular levels. Results indicated that *ApoE$^{-/-}$* mice showed a bone loss, which might be due to reduced osteogenesis. To investigate the underlying mechanisms, we used an osteoblastic differentiation culture system *in vitro* to explore the effect of *ApoE* deficiency. The result showed that *ApoE* deficiency attenuated osteogenesis *via* down-regulating osterix.

The ApoE component is a ligand for the LDL receptor, and *ApoE* deficiency increases the serum level of TC and LDL because of the failure of LDL receptor-mediated clearance (*26*). A further study proved that increased dietary lipids interfered with bone metabolism (*27*). We demonstrated osteopenia in *ApoE$^{-/-}$* mice and further focused on the impact of *ApoE* deficiency on osteoblasts. Osteoblasts were derived from pluripotent MSCs that were the progenitors of multiple types of cells (*28,29*). The osteoblastic differentiation process includes cell proliferation, extracellular matrix formation and maturation, and mineralization (*30*). Osteoblasts secrete specific extracellular matrix proteins, including osteocalcin, ALP, and collagen-1, to form bone calcium nodules (*31,32*). Our results demonstrated an indistinguishable difference between *ApoE$^{-/-}$* and WT primary osteoblasts in the proliferative activity and collagen-1 expression. Since *ApoE* did not impact osteoblast proliferation and extracellular matrix formation, we speculated that *ApoE* deficiency might hinder osteoblast differentiation or mineralization. Results showed decreased ALP activity and reduced bone calcium nodules in *ApoE$^{-/-}$* osteoblasts, suggesting that *ApoE* deficiency attenuated cell activity and inhibited mineralization of differentiated primary osteoblasts.

Osteoblasts differentiation from MSCs depends on the transcription factors Runx2 and osterix (*24*). Runx2 is essential for the differentiation of osteoblasts and can stimulate the transcription of osteocalcin, collagen-1, osteopontin, and collagenase-3 during the differentiation process of MSCs into osteoblasts (*33*). *Osterix*, a bone morphogenetic protein-induced gene, is essential for transcriptional processes in osteoblasts (*25,34*). Although Runx2 and osterix are both crucial in osteoblast differentiation, the expression of the *osterix* gene could not be detected in *Runx2$^{-/-}$* mice, indicating that osterix is downstream of Runx2 regulation and plays a vital role during the osteoblast differentiation (*24,25*). Although the mRNA level of *Runx2* in primary osteoblasts was enhanced, the mRNA expression of osterix was suppressed at the late stage of differentiation. The osterix protein level also decreased in *ApoE$^{-/-}$* osteoblasts, indicating that the down-regulated expression of osterix might contribute to the impaired osteogenesis in *ApoE*-deficient osteoblasts. Given that osteoblasts lacking *ApoE* appeared to have less osteoblastic differentiation

activity than WT osteoblasts due to reduced expression of osterix, *ApoE* may affect osterix gene expression through a Runx2 independent pathway. Further research is needed to explore the relationship between Runx2 and osterix when *ApoE* is absent and the potential mechanisms of *ApoE* regulating the osterix expression.

The interactions of osteoblasts and osteoclasts regulate bone formation and resorption (*35,36*). Communications between those two key players of bone metabolism are achieved through paracrine, direct cell-cell contact, or cell-bone matrix contact, especially the RANKL/RANK/OPG system (*35,37,38*). Osteoblasts can express OPG, a decoy RANKL receptor negatively regulating osteoclasts development (*39*). Moreover, RANKL secreted by osteoblasts can bind to RANK on the osteoclasts and stimulates osteoclastogenesis. *ApoE* deficiency did not affect *Rankl* gene expression; however, the OPG expression was down-regulated in *ApoE$^{-/-}$* osteoblasts. In addition, a study indicated that reconstitution of *ApoE$^{-/-}$OPG$^{-/-}$* mice with *ApoE$^{-/-}$OPG$^{+/+}$* bone marrow could rescue atherosclerotic lesion progression and vascular calcification (*40*). As a vascular protective factor, reduced OPG expression may result in osteopenia and hyperlipemia in *ApoE$^{-/-}$* mice. However, we cannot rule out the function of OPG on the two diseases in the *ApoE*-deficient mice now, and future experiments are required to analyze these mechanisms.

In the current study, bone loss was enhanced in *ApoE*-deficient mice after estrogen deprivation by ovariectomy, which might be due to the hindered osteogenesis *via* down-regulating osterix. The precise role of *ApoE* in the common pathomechanisms among estrogen, lipid metabolism, and bone metabolism would be an interesting question to be explored.

Conflict of Interest: The authors have no conflicts of interest to disclose.

References

1. Tian L, Yu X. Lipid metabolism disorders and bone dysfunction - interrelated and mutually regulated (review). Mol Med Rep. 2015; 12:783-794.

2. Zhang Q, Zhou J, Wang Q, Lu C, Xu Y, Cao H, Xie X, Wu X, Li J, Chen D. Association between bone mineral density and lipid profile in Chinese women. Clin Interv Aging. 2020; 15:1649-1664.

3. Silva HC, Pinheiro MM, Genaro PS, Castro CH, Monteiro CM, Fonseca FA, Szejnfeld VL. Higher prevalence of morphometric vertebral fractures in patients with recent coronary events independently of BMD measurements. Bone. 2013; 52:562-567.

4. Yang Y, Liu G, Zhang Y, Xu G, Yi X, Liang J, Zhao C, Liang J, Ma C, Ye Y, Yu M, Qu X. Association between bone mineral density, bone turnover markers, and serum cholesterol levels in type 2 diabetes. Front Endocrinol (Lausanne). 2018; 9:646.

5. Frechette DM, Krishnamoorthy D, Pamon T, Chan ME, Patel V, Rubin CT. Mechanical signals protect stem cell lineage selection, preserving the bone and muscle phenotypes in obesity. Ann N Y Acad Sci. 2017; 1409:33-50.

6. Parhami F, Jackson SM, Tintut Y, Le V, Balucan JP, Territo M, Demer LL. Atherogenic diet and minimally oxidized low density lipoprotein inhibit osteogenic and promote adipogenic differentiation of marrow stromal cells. J Bone Miner Res. 1999; 14:2067-2078.

7. King S, Klineberg I, Brennan-Speranza TC. Adipose tissue dysfunction: Impact on bone and osseointegration. Calcif Tissue Int. 2022; 110:32-40.

8. Sage AP, Lu J, Atti E, Tetradis S, Ascenzi MG, Adams DJ, Demer LL, Tintut Y. Hyperlipidemia induces resistance to PTH bone anabolism in mice *via* oxidized lipids. J Bone Miner Res. 2011; 26:1197-1206.

9. Zhang Y, Bradley AD, Wang D, Reinhardt RA. Statins, bone metabolism and treatment of bone catabolic diseases. Pharmacol Res. 2014; 88:53-61.

10. Yang TL, Shen H, Liu A, Dong SS, Zhang L, Deng FY, Zhao Q, Deng HW. A road map for understanding molecular and genetic determinants of osteoporosis. Nat Rev Endocrinol. 2020; 16:91-103.

11. Langdahl BL. Overview of treatment approaches to osteoporosis. Br J Pharmacol. 2021; 178:1891-1906.

12. Eastell R, O'Neill TW, Hofbauer LC, Langdahl B, Reid IR, Gold DT, Cummings SR. Postmenopausal osteoporosis. Nat Rev Dis Primers. 2016; 2:16069.

13. Li SS, He SH, Xie PY, Li W, Zhang XX, Li TF, Li DF. Recent progresses in the treatment of osteoporosis. Front Pharmacol. 2021; 12:717065.

14. Martin TJ, Sims NA. RANKL/OPG; critical role in bone physiology. Rev Endocr Metab Disord. 2015; 16:131-139.

15. Bos MM, Noordam R, Blauw GJ, Slagboom PE, Rensen PCN, van Heemst D. The ApoE ε4 isoform: Can the risk of diseases be reduced by environmental factors? J Gerontol A Biol Sci Med Sci. 2019; 74:99-107.

16. Schilling AF, Schinke T, Münch C, Gebauer M, Niemeier A, Priemel M, Streichert T, Rueger JM, Amling M. Increased bone formation in mice lacking apolipoprotein E. J Bone Miner Res. 2005; 20:274-282.

17. Poznyak AV, Grechko AV, Wetzker R, Orekhov AN. In search for genes related to atherosclerosis and dyslipidemia using animal models. Int J Mol Sci. 2020; 21:2097.

18. Hirasawa H, Tanaka S, Sakai A, Tsutsui M, Shimokawa H, Miyata H, Moriwaki S, Niida S, Ito M, Nakamura T. ApoE gene deficiency enhances the reduction of bone formation induced by a high-fat diet through the stimulation of p53-mediated apoptosis in osteoblastic cells. J Bone Miner Res. 2007; 22:1020-1030.

19. Wang Q, Ferreira DLS, Nelson SM, Sattar N, Ala-Korpela M, Lawlor DA. Metabolic characterization of menopause: Cross-sectional and longitudinal evidence. BMC Med. 2018; 16:17.

20. Gui Y, Chu N, Qiu X, Tang W, Gober HJ, Li D, Wang L. 17-β-estradiol up-regulates apolipoprotein genes expression during osteoblast differentiation *in vitro*. Biosci Trends. 2016; 10:140-151.

21. Qi Q, Chen L, Sun H, Zhang N, Zhou J, Zhang Y, Zhang X, Li L, Li D, Wang L. Low-density lipoprotein receptor deficiency reduced bone mass in mice *via* the c-fos/NFATc1 pathway. Life Sci. 2022; 310:121073.

22. Parfitt AM, Drezner MK, Glorieux FH, Kanis JA, Malluche H, Meunier PJ, Ott SM, Recker RR. Bone histomorphometry: Standardization of nomenclature, symbols, and units. Report of the ASBMR Histomorphometry Nomenclature Committee. J Bone Miner Res. 1987; 2:595-610.

23. Li L, Zhou J, Xu Y, Huang Z, Zhang N, Qiu X, Wang L. C-C chemokine receptor type 6 modulates the biological function of osteoblastogenesis by altering the expression levels of osterix and OPG/RANKL. Biosci Trends. 2021; 15:240-248.

24. Chan WCW, Tan Z, To MKT, Chan D. Regulation and role of transcription factors in osteogenesis. Int J Mol Sci. 2021; 22:5445.

25. Nakashima K, Zhou X, Kunkel G, Zhang Z, Deng JM, Behringer RR, de Crombrugghe B. The novel zinc finger-containing transcription factor osterix is required for osteoblast differentiation and bone formation. Cell. 2002; 108:17-29.

26. Zhang SH, Reddick RL, Piedrahita JA, Maeda N. Spontaneous hypercholesterolemia and arterial lesions in mice lacking apolipoprotein E. Science. 1992; 258:468-471.

27. Li H, Gou Y, Tian F, Zhang Y, Lian Q, Hu Y, Zhang L. Combination of metformin and exercise alleviates osteoarthritis in ovariectomized mice fed a high-fat diet. Bone. 2022; 157:116323.

28. Wang C, Wang Y, Meng HY, Yuan XL, Xu XL, Wang AY, Guo QY, Peng J, Lu SB. Application of bone marrow mesenchymal stem cells to the treatment of osteonecrosis of the femoral head. Int J Clin Exp Med. 2015; 8:3127-3135.

29. Chamberlain G, Fox J, Ashton B, Middleton J. Concise review: Mesenchymal stem cells: Their phenotype, differentiation capacity, immunological features, and potential for homing. Stem Cells. 2007; 25:2739-2749.

30. Ponzetti M, Rucci N. Osteoblast differentiation and signaling: Established concepts and emerging topics. Int J Mol Sci. 2021; 22:6651.

31. Blair HC, Larrouture QC, Li Y, Lin H, Beer-Stoltz D, Liu L, Tuan RS, Robinson LJ, Schlesinger PH, Nelson DJ. Osteoblast differentiation and bone matrix formation *in vivo* and *in vitro*. Tissue Eng Part B Rev. 2017; 23:268-

280.

32. Lin X, Patil S, Gao YG, Qian A. The bone extracellular matrix in bone formation and regeneration. Front Pharmacol. 2020; 11:757.

33. Ducy P, Zhang R, Geoffroy V, Ridall AL, Karsenty G. Osf2/Cbfa1: A transcriptional activator of osteoblast differentiation. Cell. 1997; 89:747-754.

34. Zhang C. Transcriptional regulation of bone formation by the osteoblast-specific transcription factor Osx. J Orthop Surg Res. 2010; 5:37.

35. Yuan FL, Wu QY, Miao ZN, Xu MH, Xu RS, Jiang DL, Ye JX, Chen FH, Zhao MD, Wang HJ, Li X. Osteoclast-derived extracellular vesicles: Novel regulators of osteoclastogenesis and osteoclast-osteoblasts communication in bone remodeling. Front Physiol. 2018; 9:628.

36. Chen X, Wang Z, Duan N, Zhu G, Schwarz EM, Xie C. Osteoblast-osteoclast interactions. Connect Tissue Res. 2018; 59:99-107.

37. Li D, Liu J, Guo B, *et al*. Osteoclast-derived exosomal miR-214-3p inhibits osteoblastic bone formation. Nat Commun. 2016; 7:10872.

38. Xian L, Wu X, Pang L, *et al*. Matrix IGF-1 maintains bone mass by activation of mTOR in mesenchymal stem cells. Nat Med. 2012; 18:1095-1101.

39. Yao Z, Getting SJ, Locke IC. Regulation of TNF-induced osteoclast differentiation. Cells. 2021; 11:132.

40. Callegari A, Coons ML, Ricks JL, Yang HL, Gross TS, Huber P, Rosenfeld ME, Scatena M. Bone marrow- or vessel wall-derived osteoprotegerin is sufficient to reduce atherosclerotic lesion size and vascular calcification. Arterioscler Thromb Vasc Biol. 2013; 33:2491-2500.

[§]These authors contributed equally to this work.
Address correspondence to:
Yan Sun, Laboratory for Reproductive Immunology, Obstetrics and Gynecology Hospital of Fudan University, 419 Fangxie Road, 200011 Shanghai, China.
E-mail: ysunsh@126.com

Ling Wang, Laboratory for Reproductive Immunology, Obstetrics and Gynecology Hospital of Fudan University, 419 Fangxie Road, 200011 Shanghai, China.
E-mail: Dr.wangling@fudan.edu.cn